artificial intelligence for space weather forecasting: data-driven and physics-informed approaches in research and operational settings

the MIDA group
dipartimento di matematica università di genova
osservatorio astrofisico di torino, INAF

michele piana

MCH23

sofia, bulgaria
april, 19th 2023

Università di Genova

machine learning in space weather prediction

four crucial issues:

- define a validation strategy for machine/deep learning
- account for the solar cycle phase in the training and validation steps
- reduce the overall computational burden
- design physics-informed algorithms

validation

validation strategy: (guastavino et al, astronomy and astrophysics, 2022)

generation of well-balanced training, validation and test sets:

- chronological splitting introduces a bias due to the cyclicity of the solar activity
- data generation process based on machine learning theory: **training, validation and test sets must be drawn from the same distribution** (vapnik, 1998)

bootstrap analysis:

- many classification tests performed by generating many triples of training, validation and test sets
- random extraction of AR images from the HMI archive (BUT while keeping AR separation in training, validation and test)
- confidence intervals for the skill scores

data set generation

definition of data samples:

- X, M, C class
- NO1, NO2, NO3, NO4

well-balanced training and validation sets:

- **proportionality:** same rates of samples for each sample type
- **parsimony:** each subset of samples made by as few ARs as possible (i.e., samples belonging to the same AR fall into the same data set)

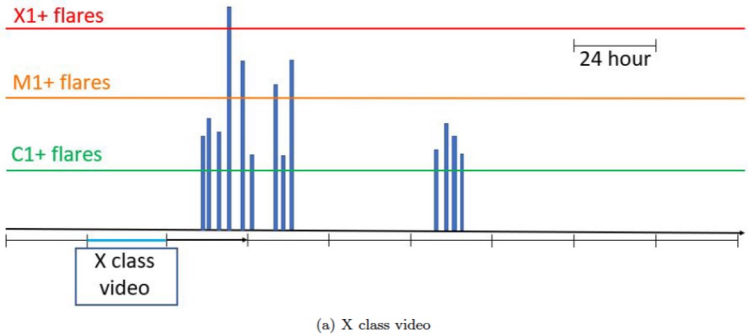

(a) X class video

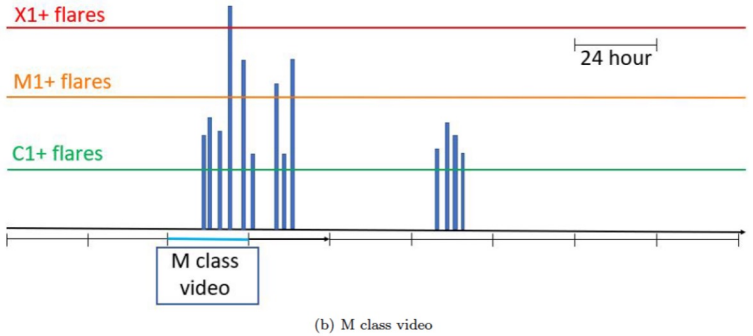

(b) M class video

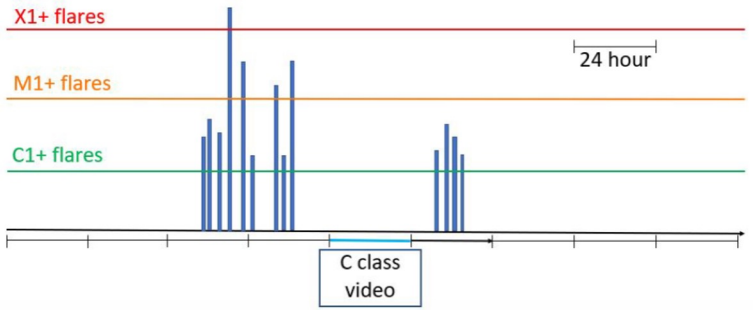

(c) C class video

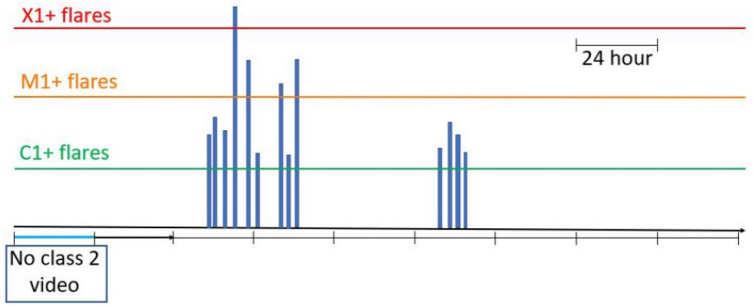

(a) No class 2 video

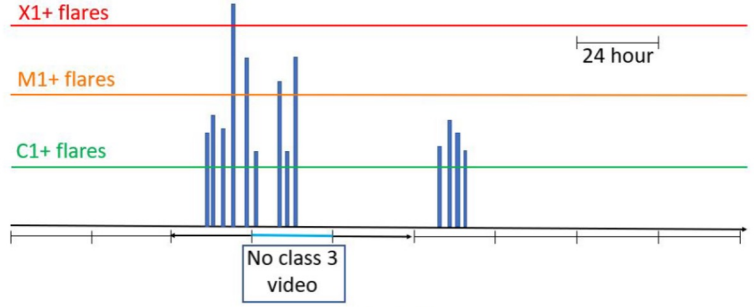

(b) No class 3 video

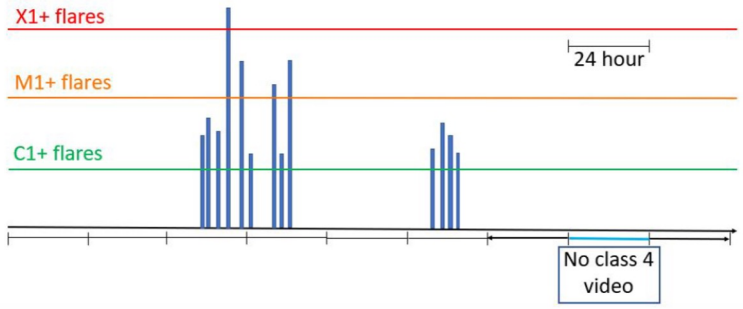

(c) No class 4 video

data

SDO/HMI images recorded in the time range between
2012 September 14 and 2017 September 30

- for each AR, we considered the HMI magnetogram frames associated to it and we organized them in 24 hour long time series of HMI magnetogram frames
- we constructed a collection of data samples, each one represented by a video of HMI magnetogram frames associated to an AR
- data from the past: we annotated each time series with 0 if no flare occurred within 24 hours and with 1 if a flare occurred within 24 hours;
- we generated 10 training, validation and test sets according to the data generation process in order to assess the statistical robustness in results

deep neural network architecture

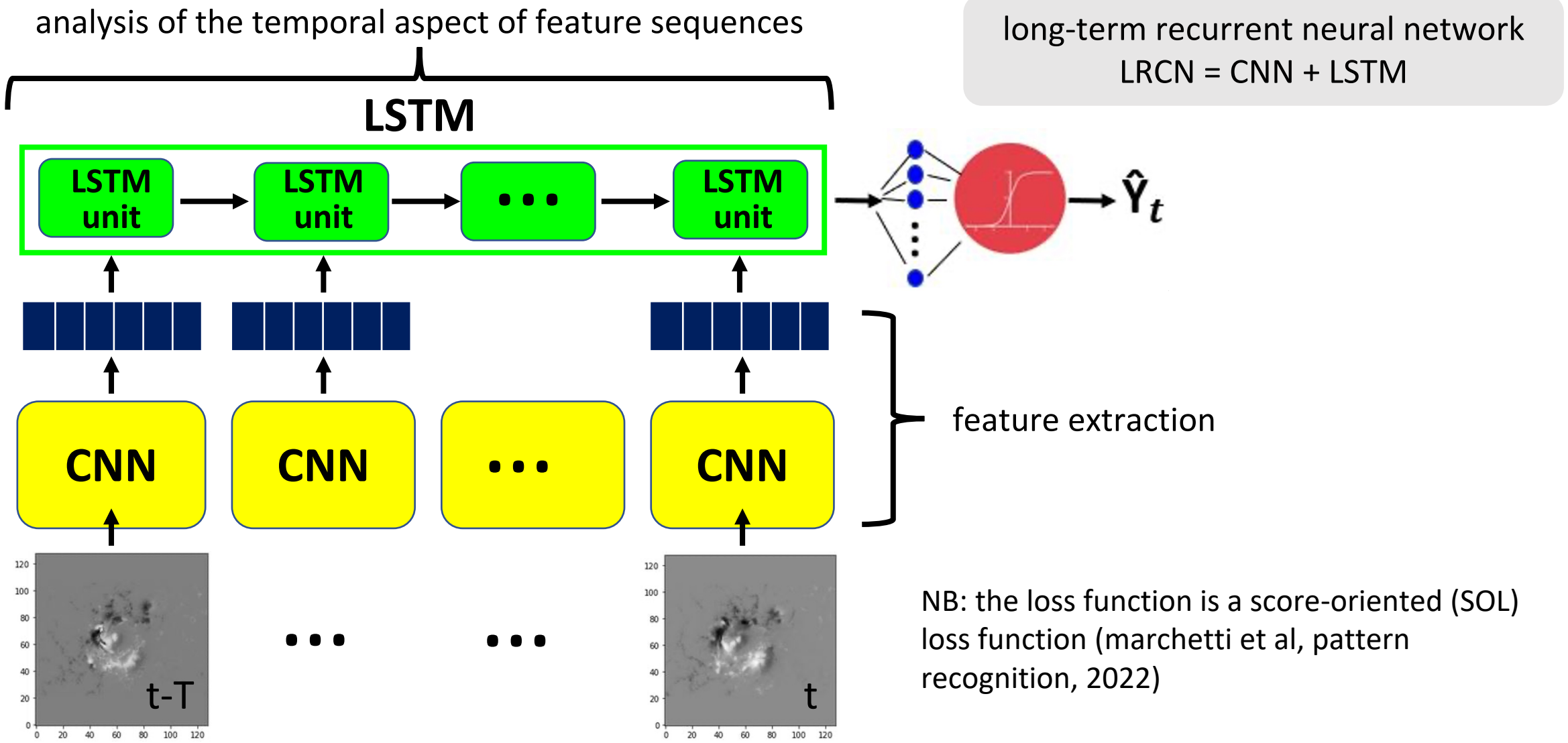

long-term recurrent neural network
LRCN = CNN + LSTM

NB: the loss function is a score-oriented (SOL) loss function (marchetti et al, pattern recognition, 2022)

results on test sets: C+ flare prediction

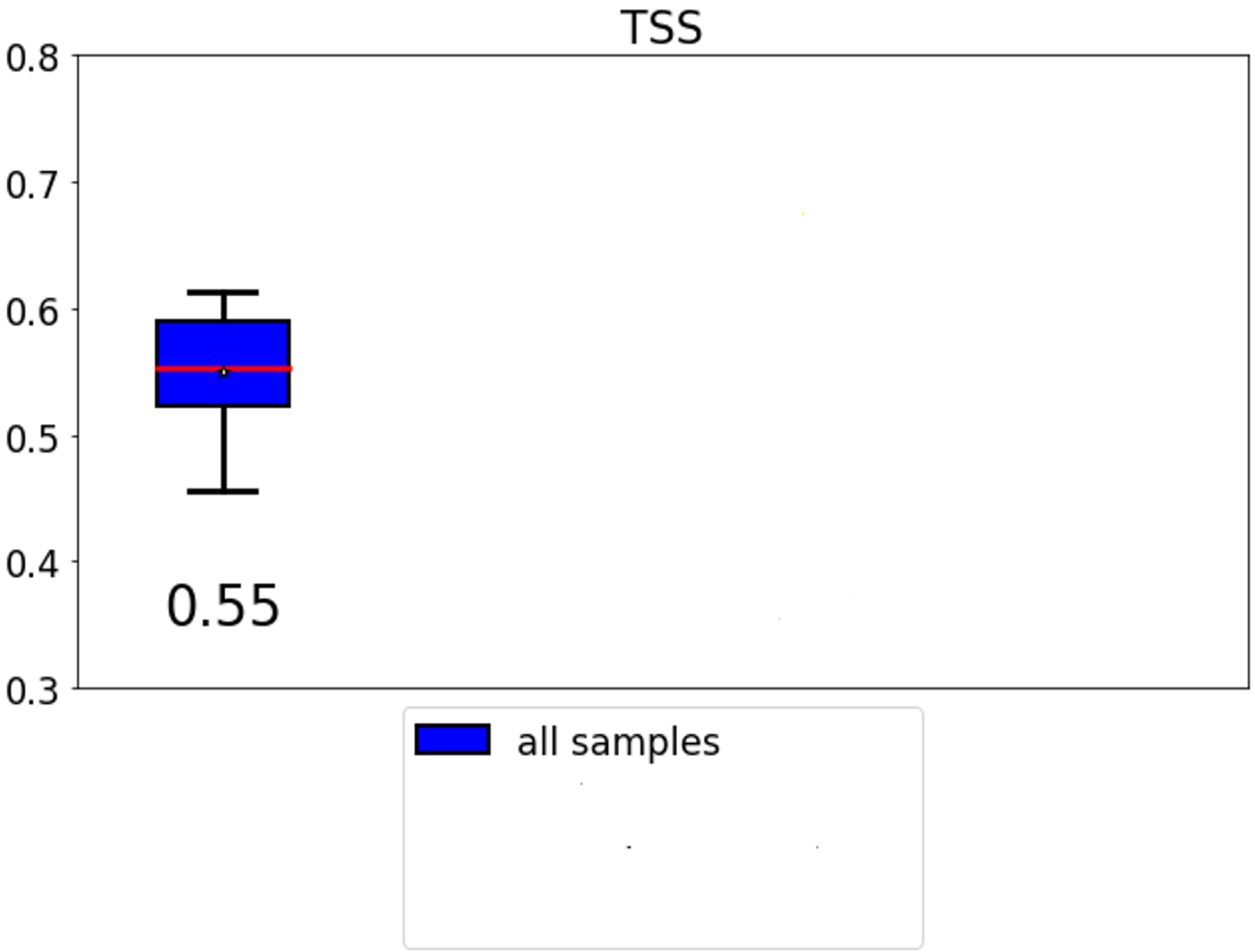

results on test sets: C+ flare prediction

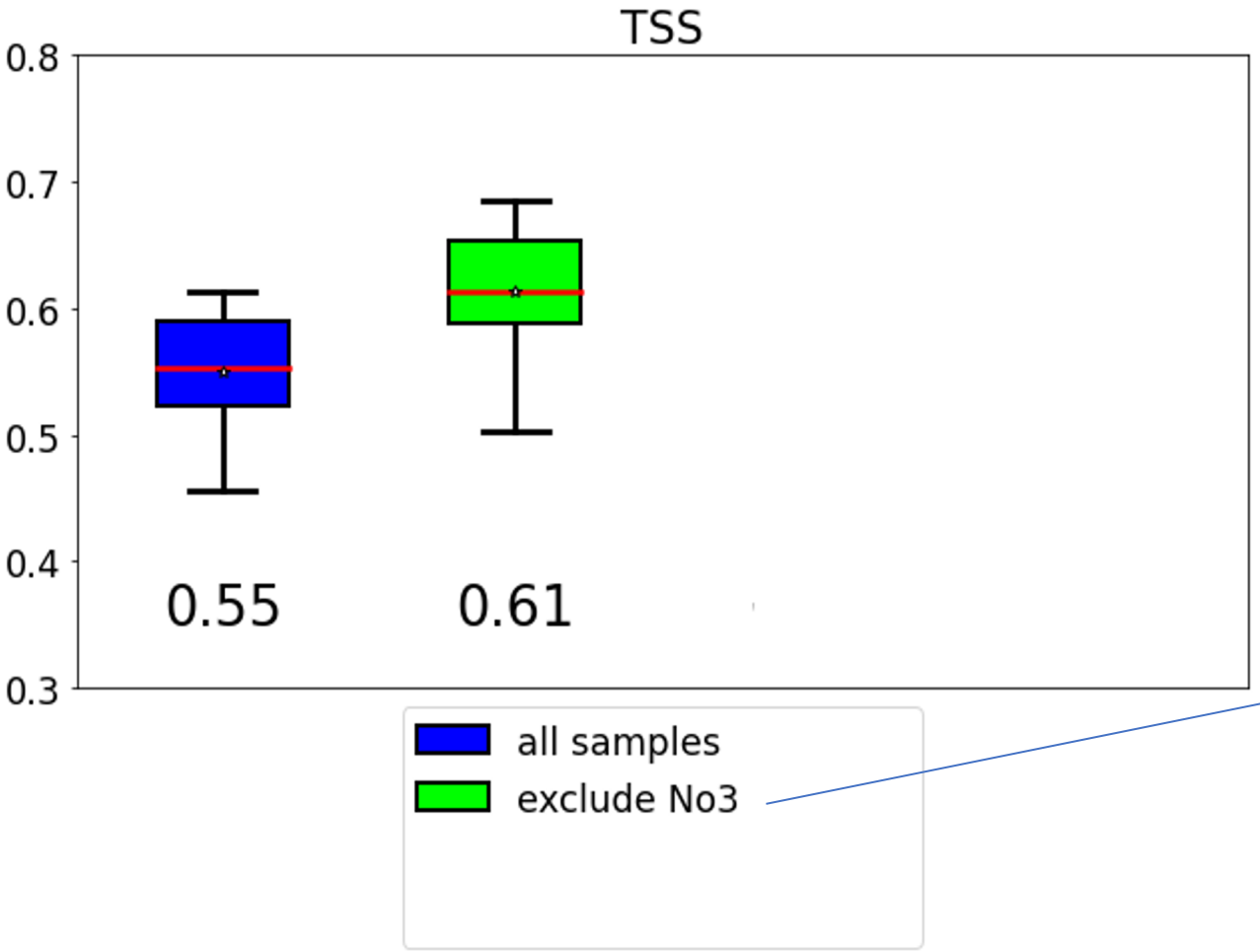

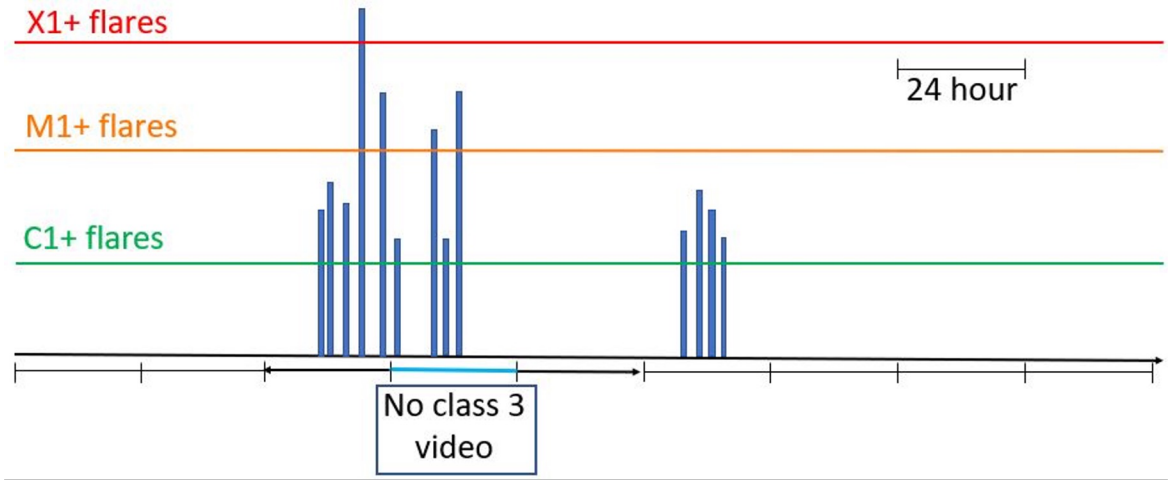

results on test sets: C+ flare prediction

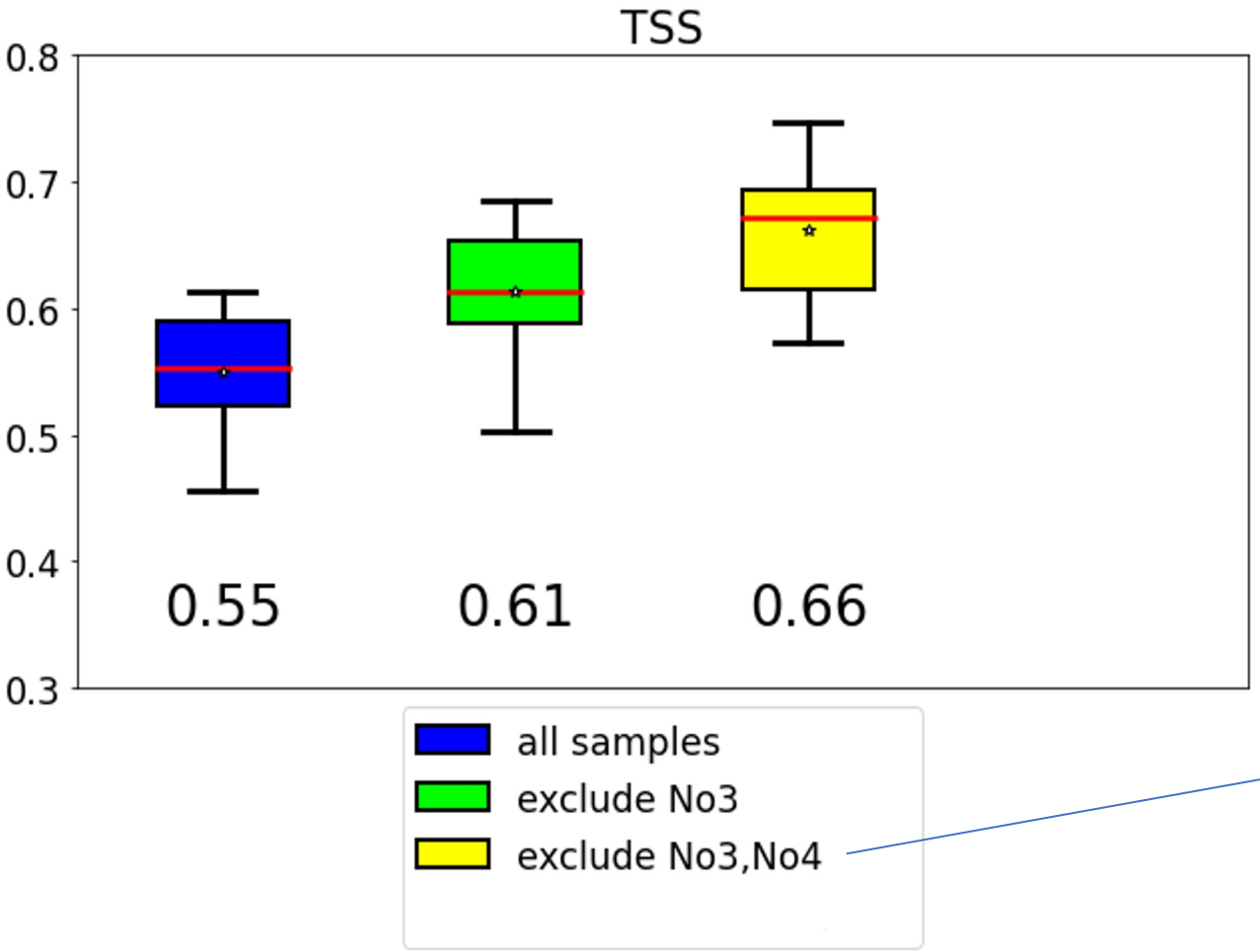

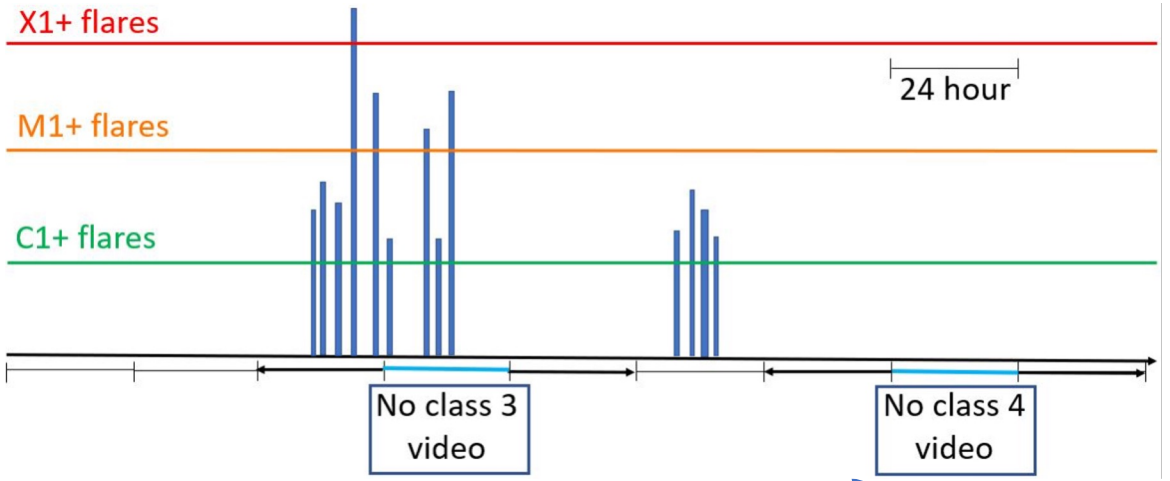

results on test sets: C+ flare prediction

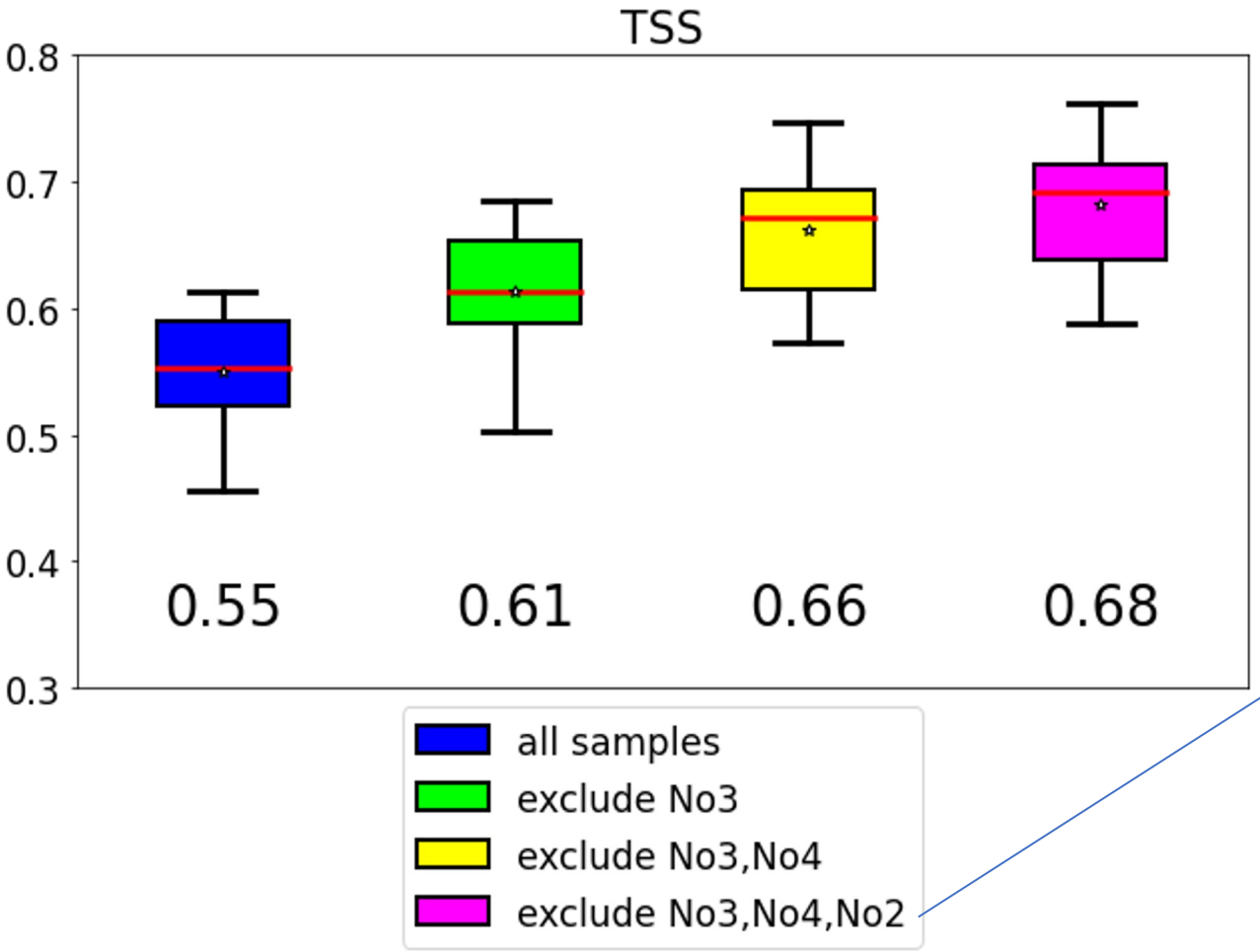

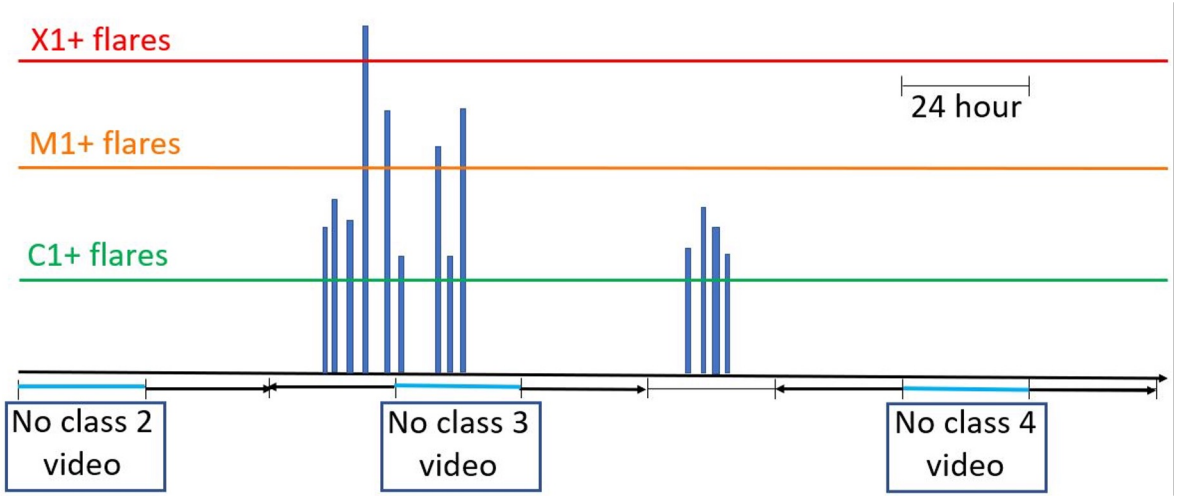

results on test sets: M+ flare prediction

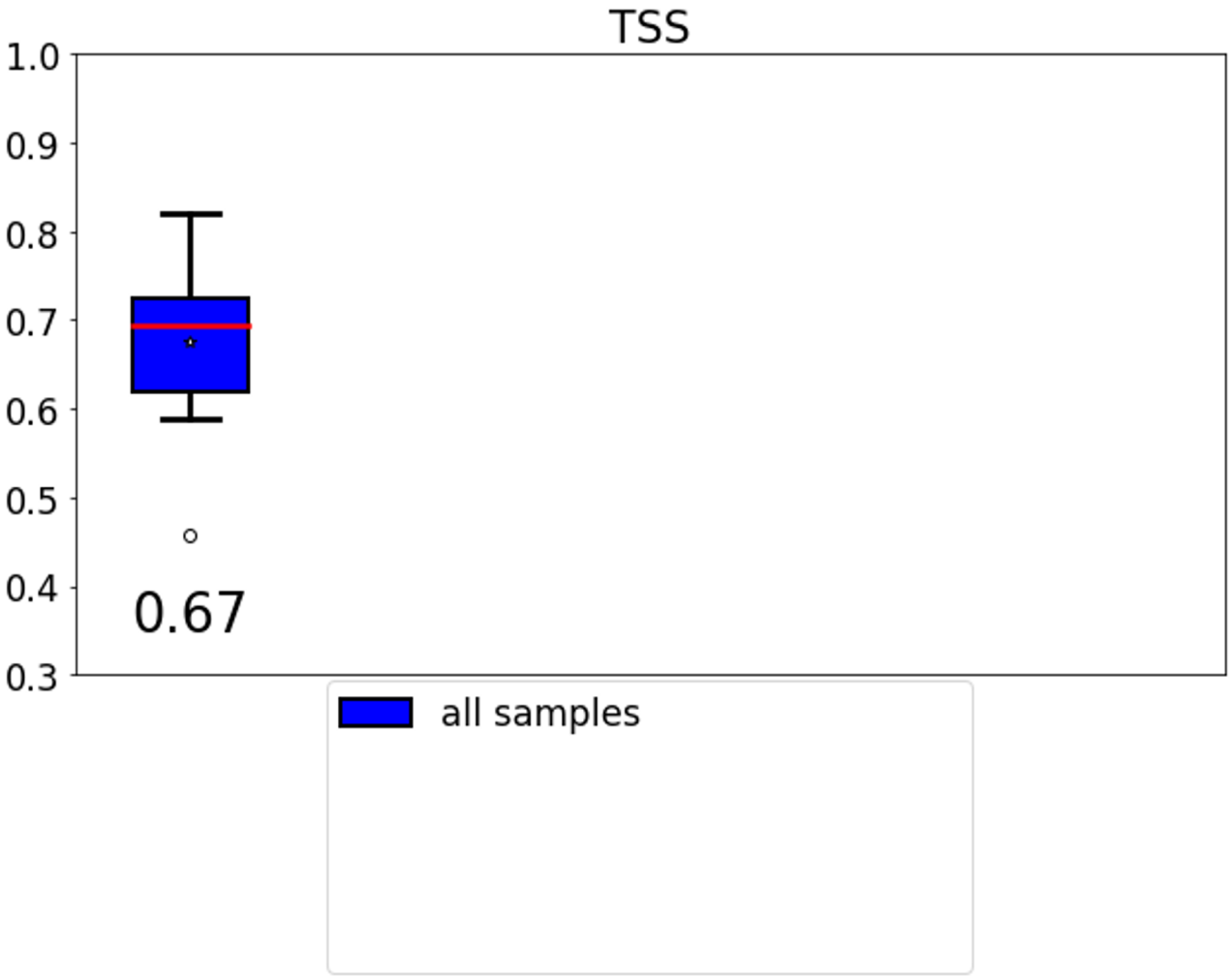

results on test sets: M+ flare prediction

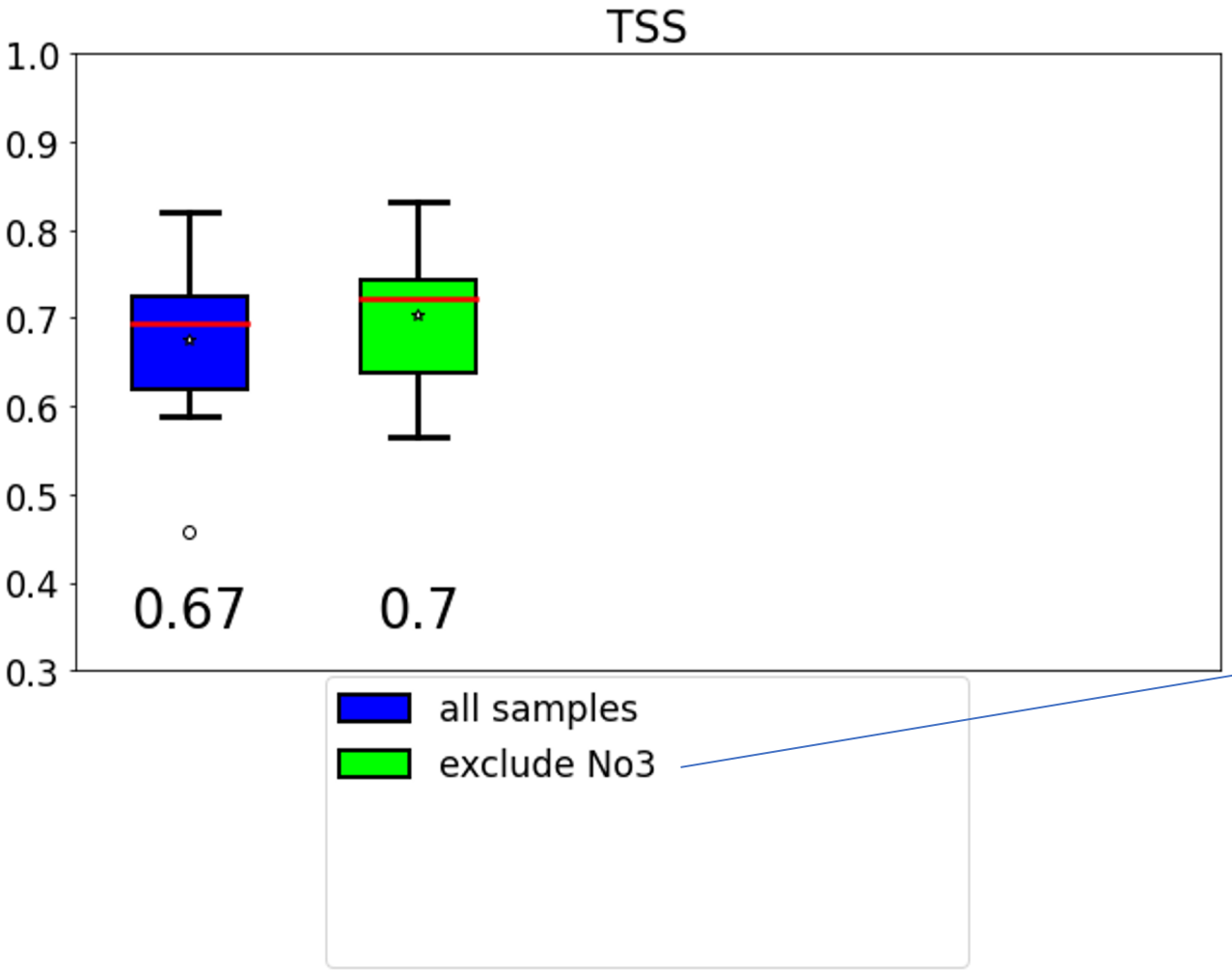

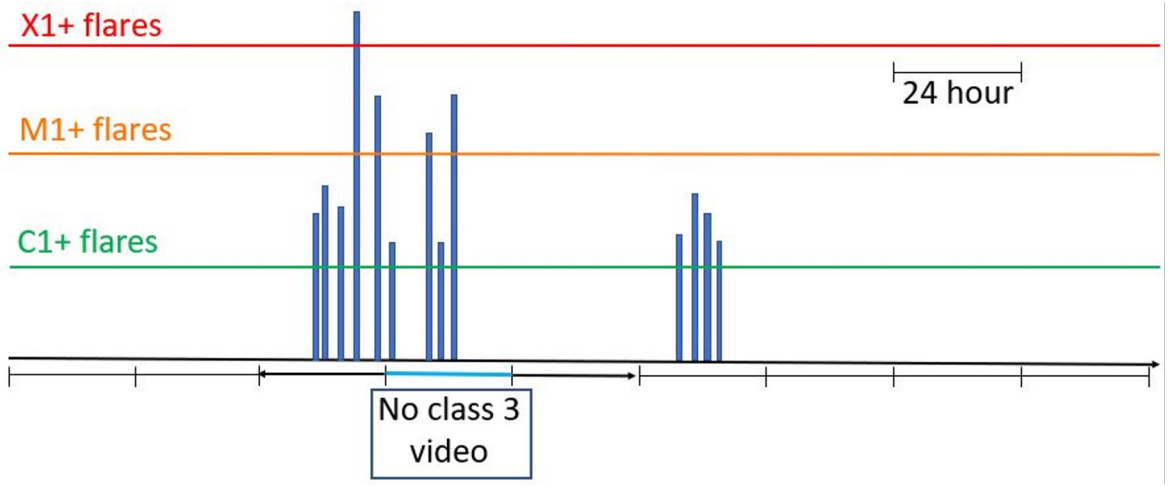

results on test sets: M+ flare prediction

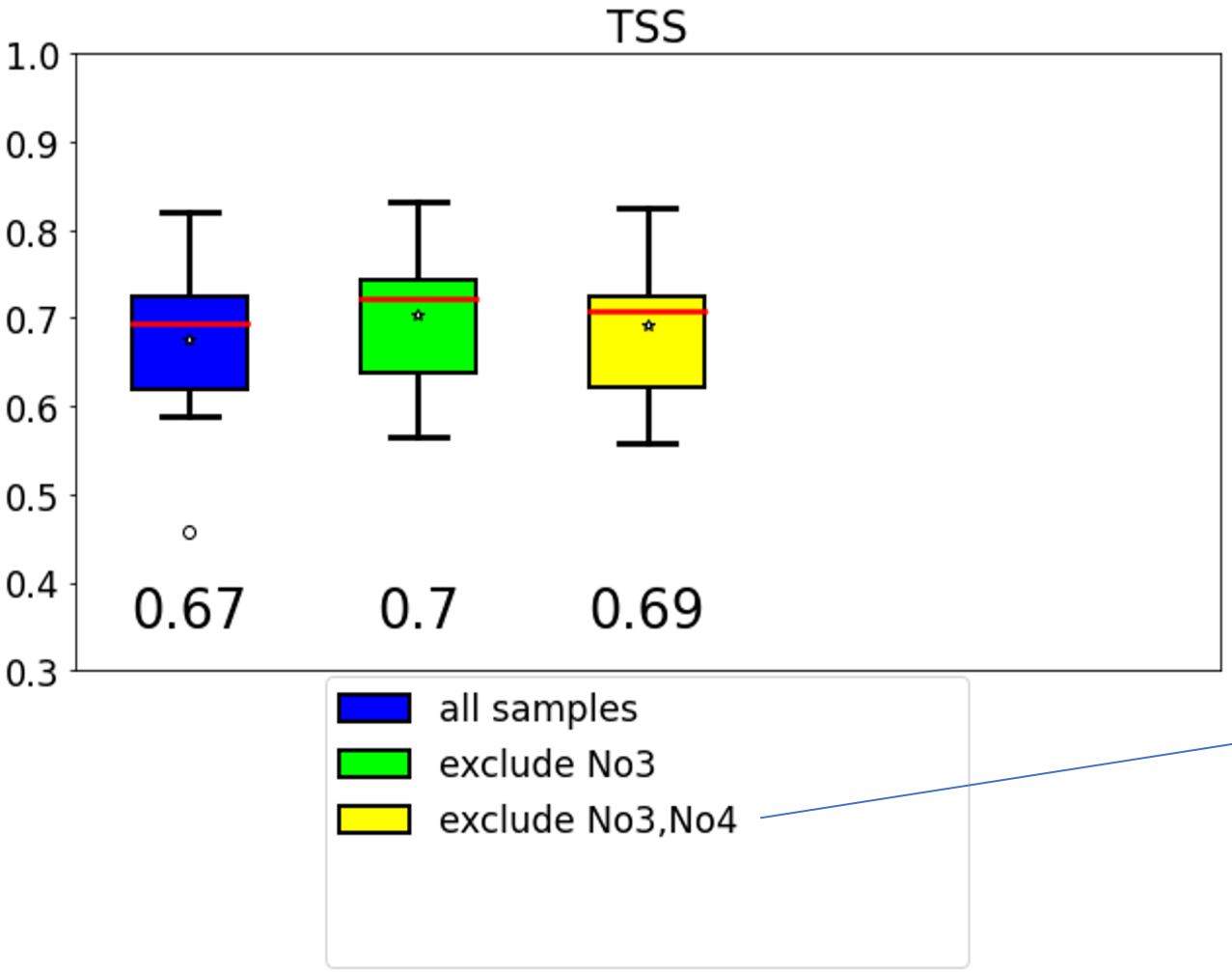

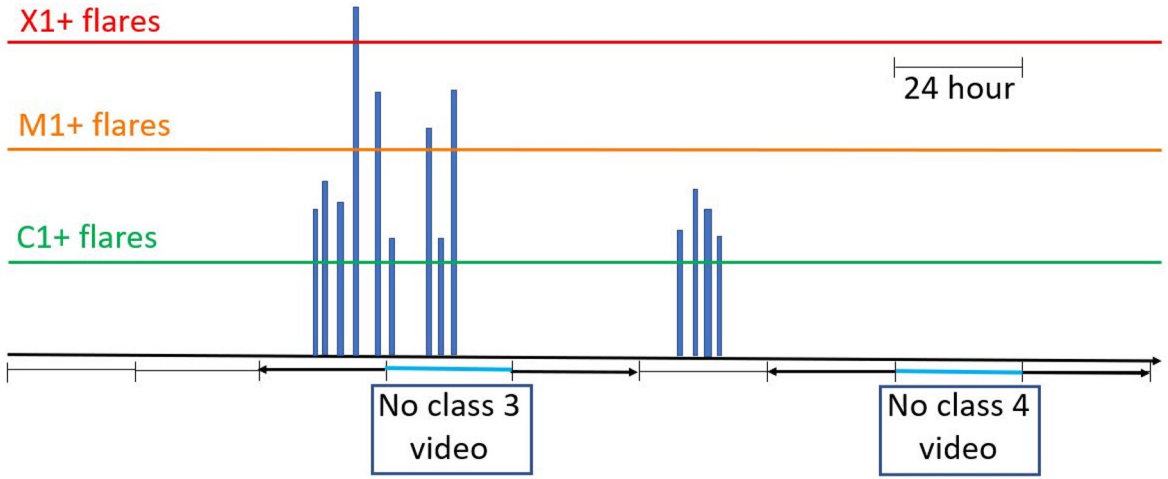

results on test sets: M+ flare prediction

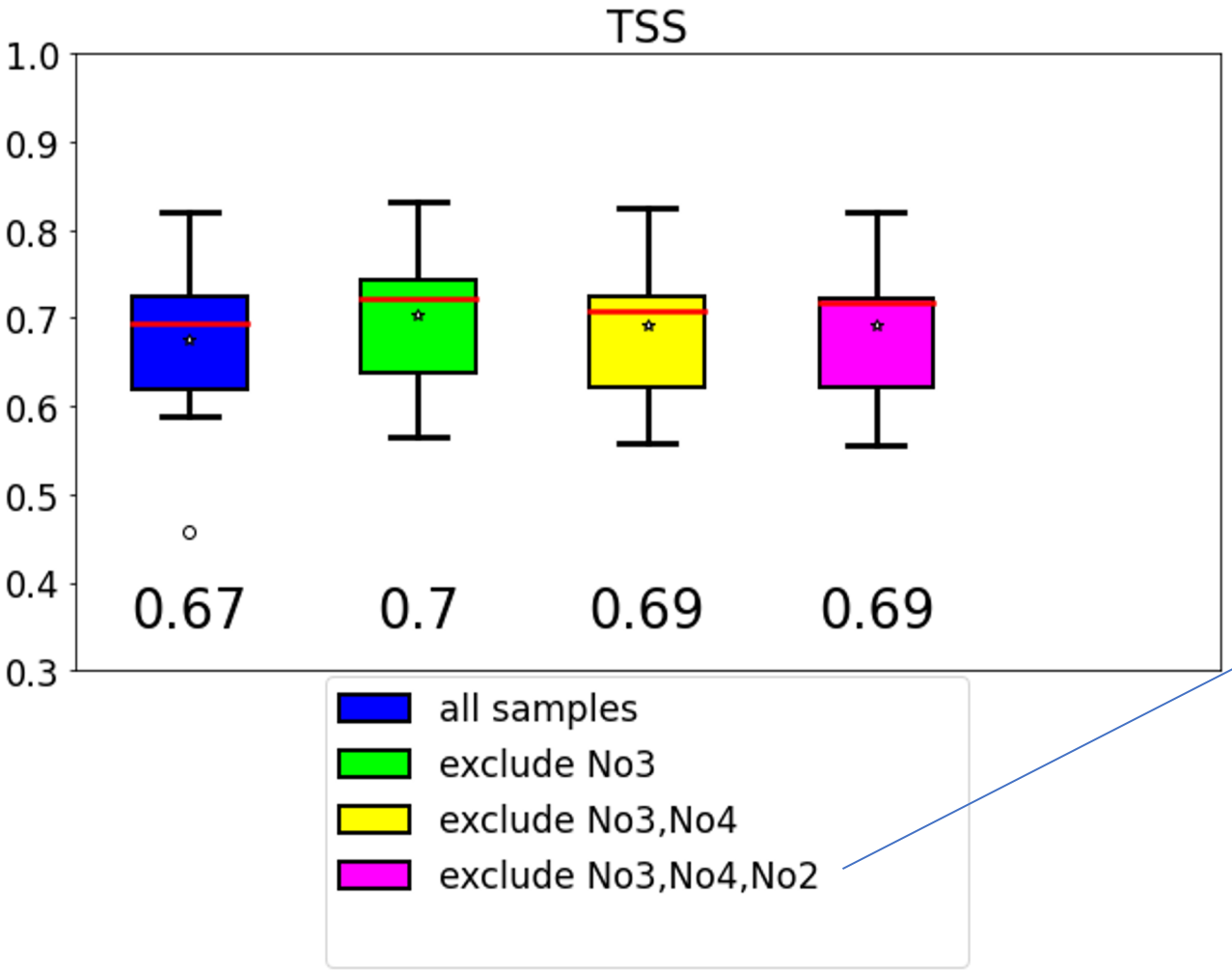

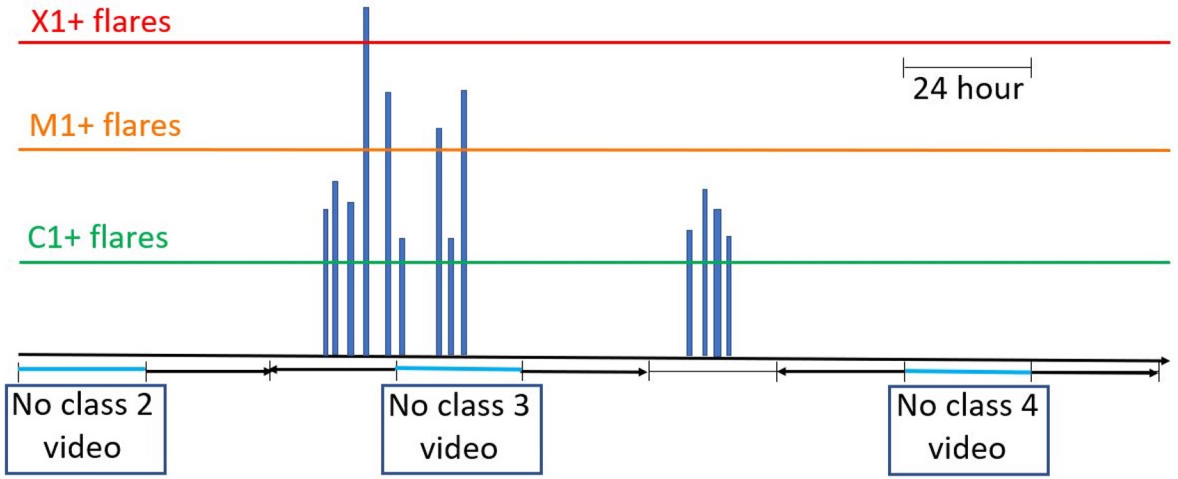

results on test sets: M+ flare prediction

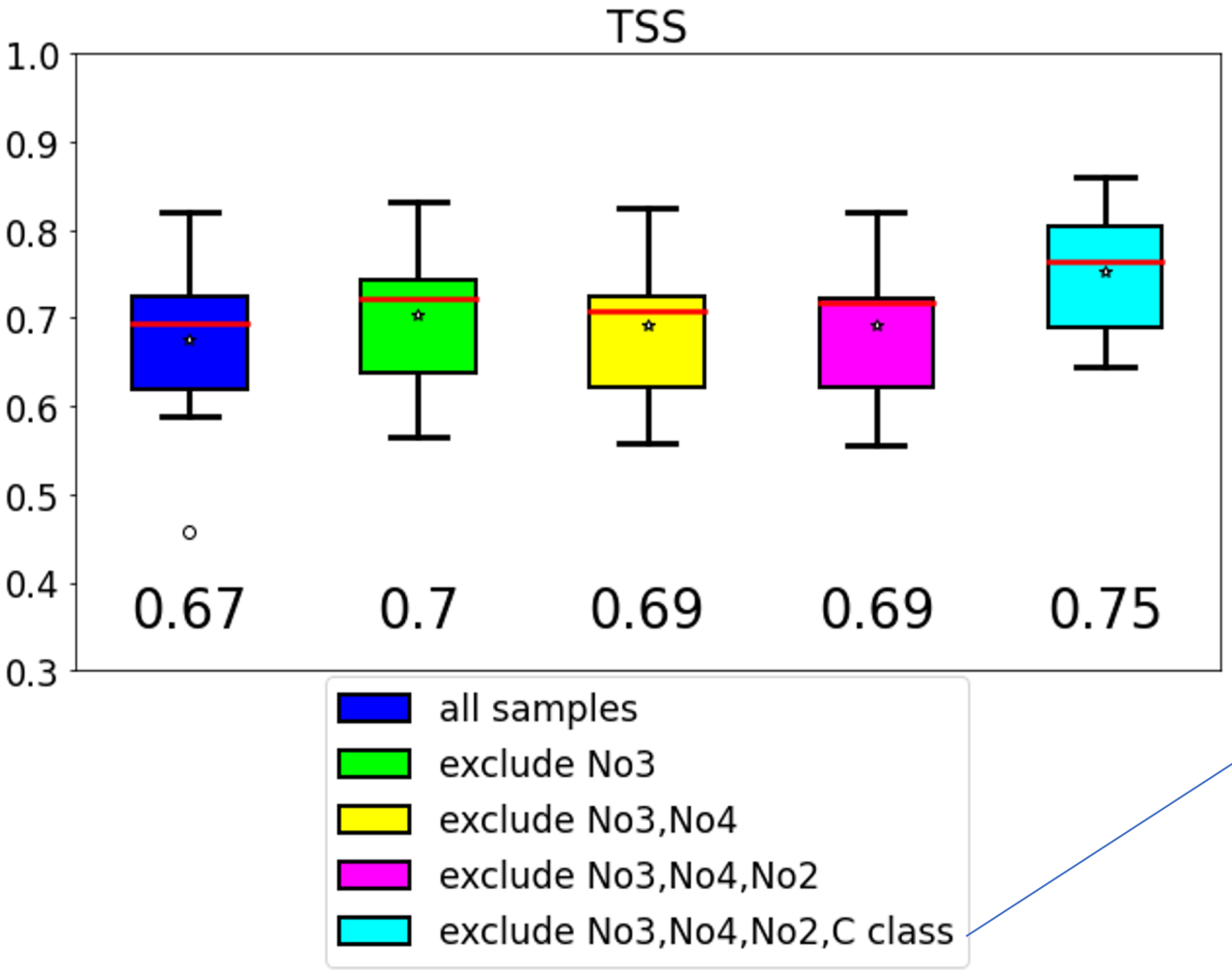

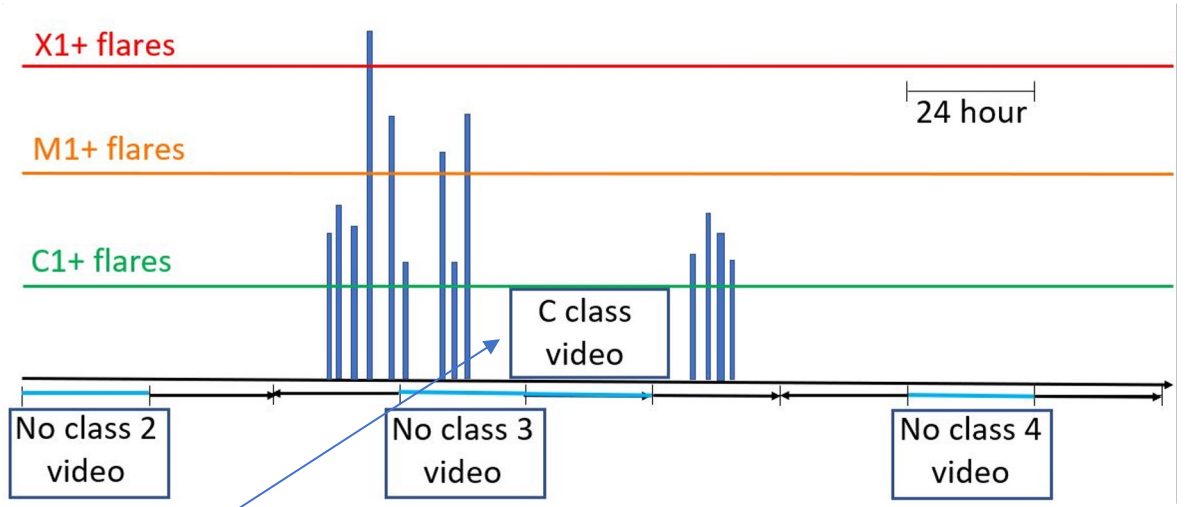

focus on solar cycle

generalization of the operational flare forecasting process

- identification of three phases in the current solar cycle: increasing, plateau, decreasing

- given a time window in the current solar cycle, the corresponding phase is identified.

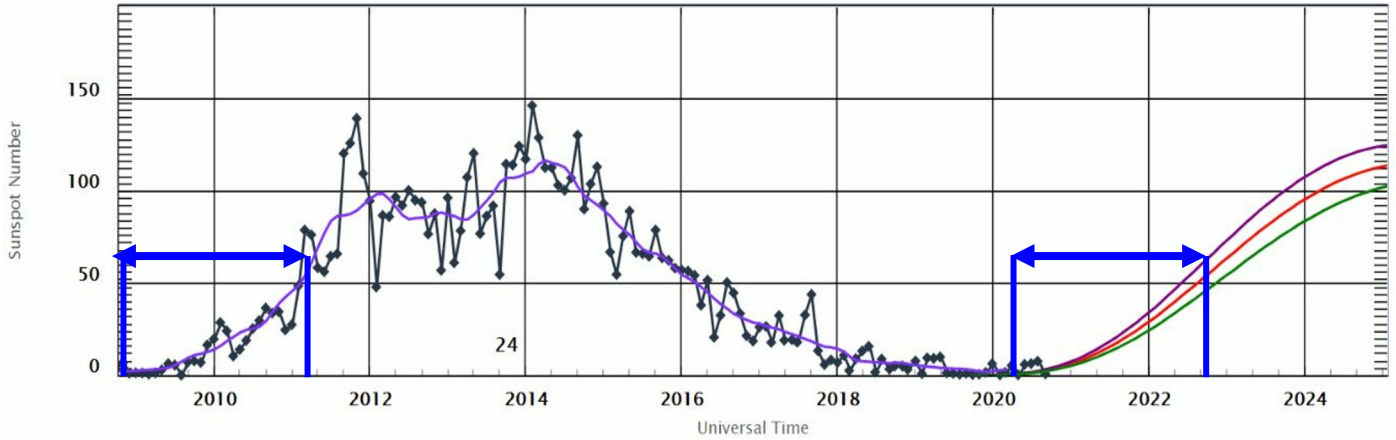

- for the same phase in the previous solar cycle the data set generation algorithm computes the rates of the different sample types

- the training and validation sets are generated according to the sample rates from the whole data archive at disposal

results: C+ flare prediction (guastavino et al, frontiers in astronomy, 2023)

test window: march-december 2015 (decreasing phase)

training and validation sets are generated with the sample rates computed on the **same phase** and on the **plateau**

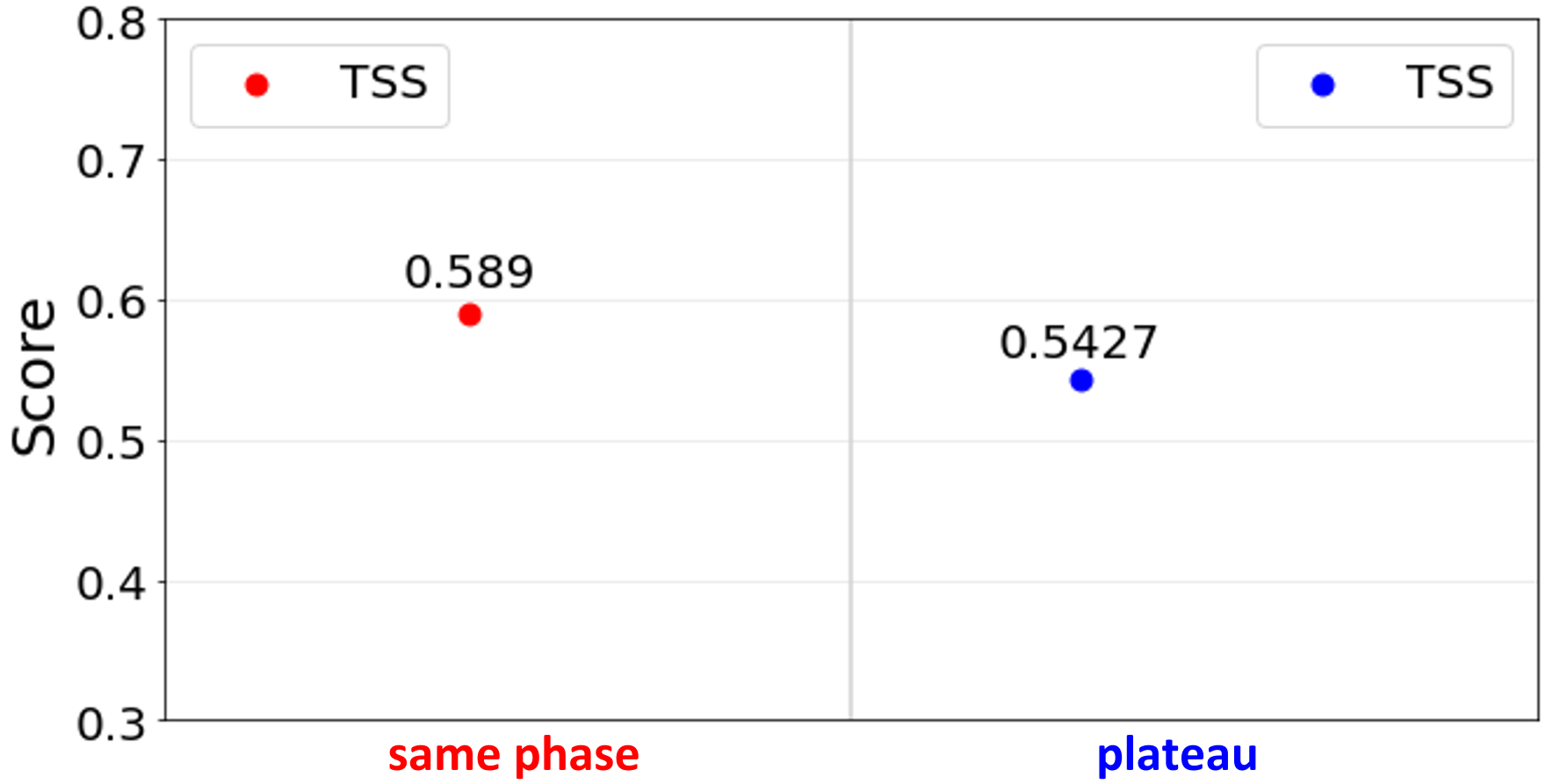

results: M+ flare prediction (guastavino et al, frontiers in astronomy, 2023)

test window: march-december 2015

training and validation sets are generated with the sample rates computed on the **same phase** or **different phase**

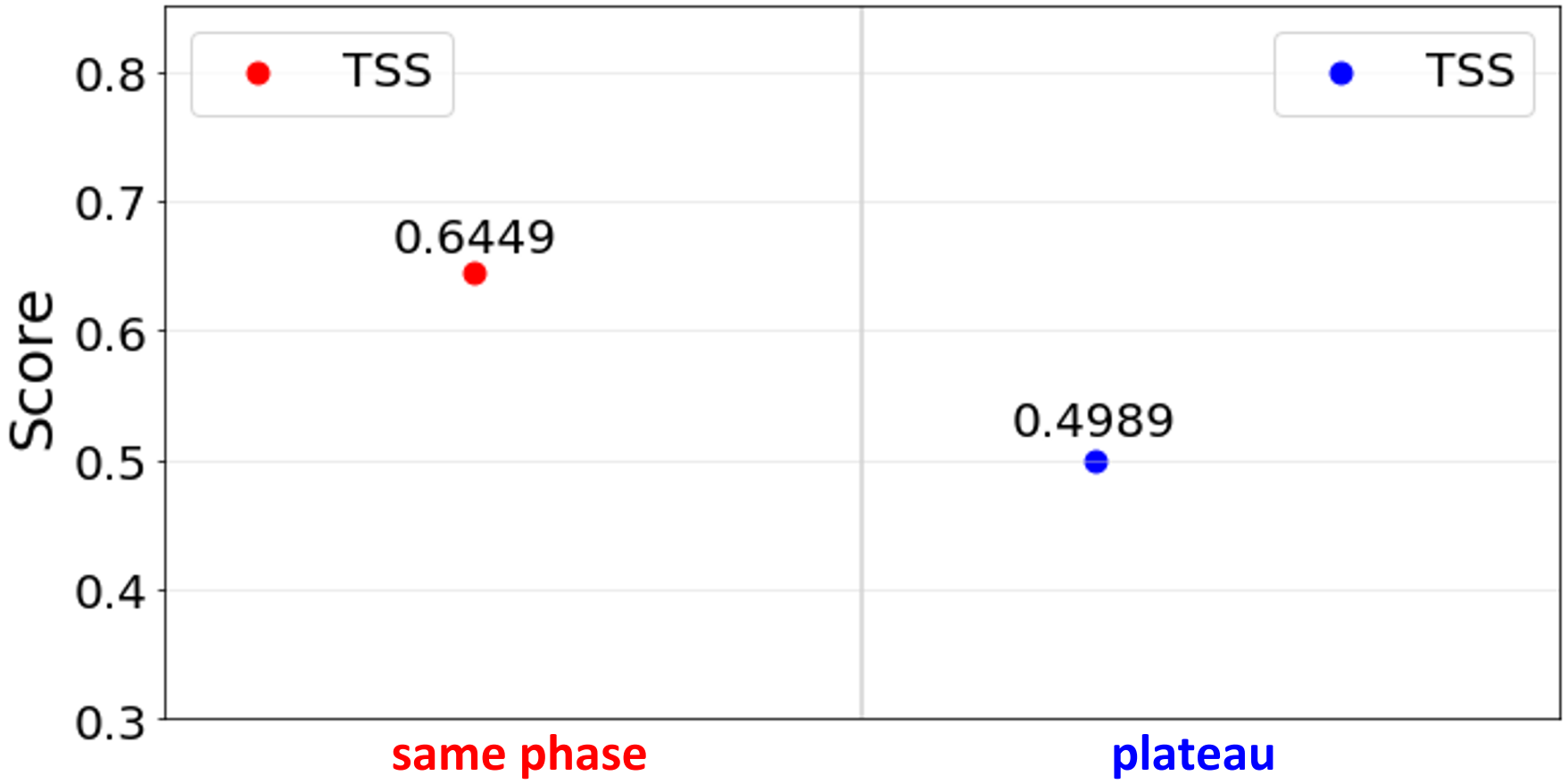

computational issues

online training: machine learning vs CNNs

- feature-based machine learning is computationally more effective for online training than image-based deep learning
- sparsity enhancing algorithms allow the identification of the image features that mostly impact the flare forecasting performances

nice piece of news (campi et al, astrophysical journal, 2019):

- rather few features contribute to the prediction process
- such features depend on neither the machine learning algorithm nor the issuing time

feature-based experiment

point-in-time SHARP images:

- time range: 09/14/2012 – 04/30/2016
- four issuing times: 00:00 UT – 06:00 UT – 12:00 UT – 18:00 UT
- cadence: 24 hours

features (for each AR):

- 171 features identified in each active region:
  - 167 extracted with a specific pattern recognition algorithms
  - longitude and latitude of the AR
  - binary label encoding the presence of a flare in the past
  - flare class (if occured)
- overall 4442 sets of 171-dimension feature vectors (one AR may last for more than one HMI image)

(the FLARECAST project: georgoulis et al, JSWSC, 2021)

different algorithms

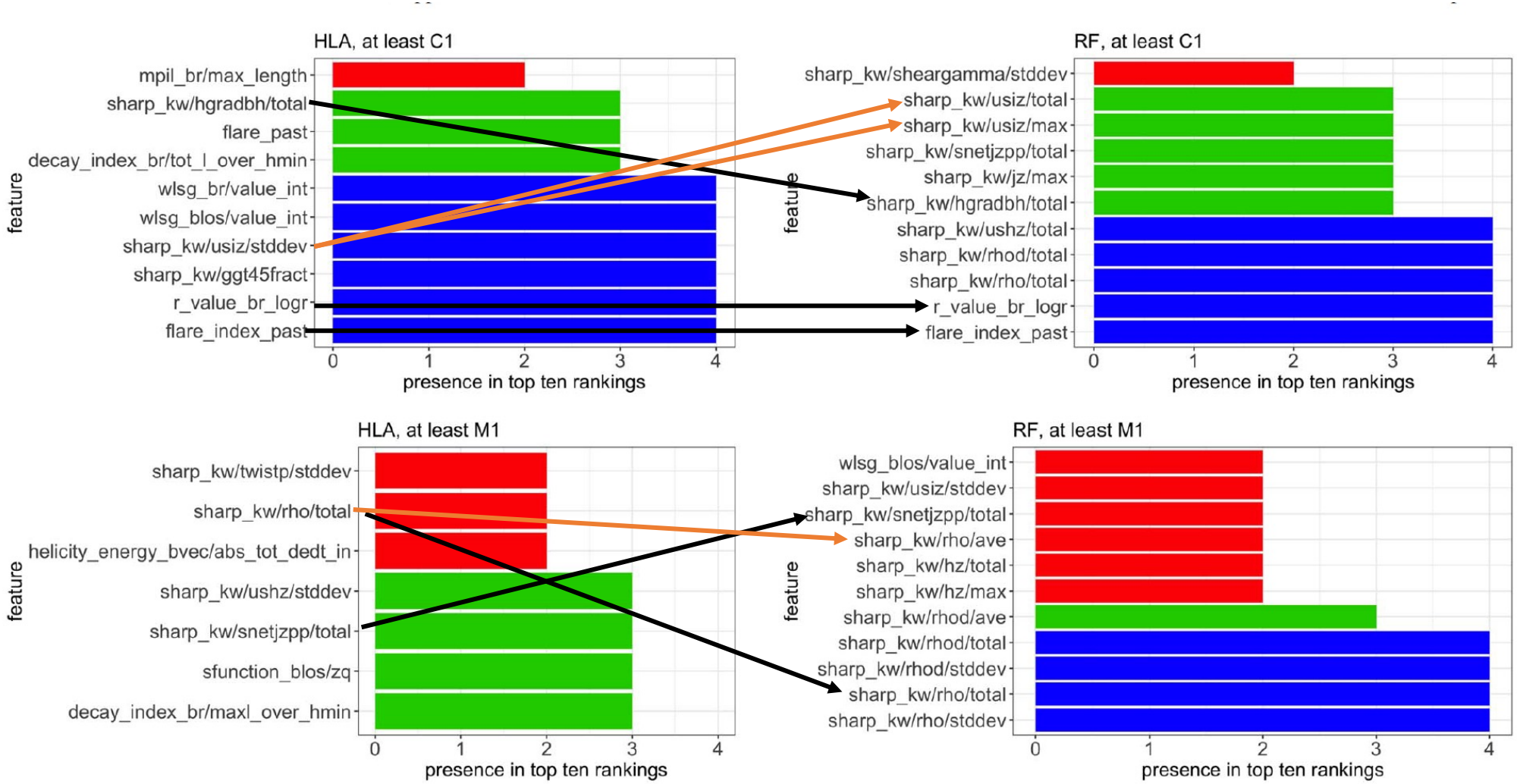

different issuing times

	at least C1 flares					
	Hybrid Lasso	Hybrid Logit	SVC	Random Forest	average	std
flare_index_past	13,08	28,84	19,91	3,51	16,56	10,63
sharp_kw/hgradbh/total	3,47	37	18,59	16,57	18,95	13,87
wlsg_br/value_int	3,74	14,43	22,86	43,14	21,04	16,68
sharp_kw/jz/max	26,05	28	16,94	18,58	22,27	5,29
sharp_kw/usiz/max	24,2	36,75	34,79	18,37	28,53	8,73
wlsg_blos/value_int	3,96	45	46,61	25,39	30,24	20,00
r_value_br_logr	3,52	2,81	128,91	7,47	35,68	62,19
sharp_kw/ggt45fract	14,99	32	57,6	49,3	38,47	19,00
sharp_kw/usiz/stddev	17,15	49,46	54,26	45,89	41,69	16,72
sharp_kw/gamma/total	61,65	20,76	52,95	34,67	42,51	18,35

issuing time: 12:00:00

	at least C1 flares					
	Hybrid Lasso	Hybrid Logit	SVC	Random Forest	average	std
wlsg_br/value_int	3,23	5	23,95	30,02	15,55	13,45
flare_index_past	13,89	31,13	33,92	5,47	21,10	13,68
sharp_kw/usiz/total	36,44	15,8	11,39	26,1	22,43	11,19
sharp_kw/hgradbh/total	29,06	7,55	24,87	39,45	25,23	13,29
sharp_kw/ggt45fract	5,25	17,14	50,68	28,25	25,33	19,33
ising_energy_br/ising_energy	24,14	19,67	26,49	55,1	31,35	16,08
wlsg_blos/value_int	12,83	35,08	41,12	51,11	35,04	16,21
r_value_br_logr	6,52	4,13	126,06	16,87	38,40	58,70
sharp_kw/usiz/stddev	4,67	22,41	69,63	57,61	38,58	30,21
sharp_kw/usiz/max	31,77	44,87	80,57	19,66	44,22	26,33

issuing time: 00:00:00

redundancy of information

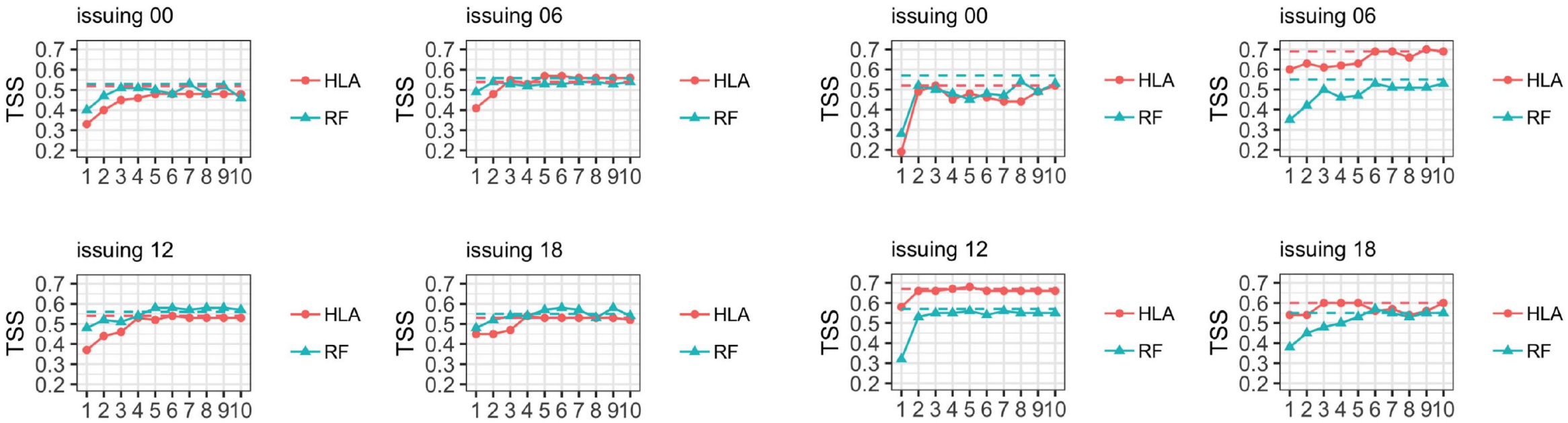

TSS scores obtained by using just the 10 top-ten features added one at a time

physics-driven machine learning

physics and machine learning

approach 1 - data-driven AI to constrain the parameters contained in MHD equations

approach 2 - physics models to improve the training phase for AI algorithms:

- encode the model equation into a (differentiable) loss function
- estimate the equation parameters by means of either physics or machine learning

example: prediction of CME's travel time

input data:

- CME's kinematic parameters measured by remote sensing instruments
- solar wind parameters measured by in-situ instruments

physics: drag-based model

unknown: CME's travel time from onset to earth

prediction of CME's travel time

Name	Notation	Unity	Description	Source
CME height of eruption	r_0	km	$r_0 = 20R_\odot$, $R_\odot = 6.957 \cdot 10^5$ km	-
CME time of eruption	t_0	s	eruption time on the Sun at r_0	LASCO
CME Time of Arrival	ToA	s	estimated arrival time at 1 AU	R & C?
CME Travel time	TT	s	estimated time between t_0 and ToA	R & C, LASCO?
CME initial speed	v_0	km/s	initial propagation speed from eruption	LASCO
CME mass	m	g	estimated CME mass	LASCO
CME impact area	A	km^2	CME impact area, constant angular width	LASCO
Solar wind density	ρ	g/km^3	mean over one hour after t_0	CELIAS
Solar wind speed	w	km/s	mean over one hour after t_0	CELIAS
Drag parameter	C	dimensionless	parameter of the drag based model	this work

experimental data

drag-based model

$$\ddot{r}(t) = -C\frac{A\rho}{m}|\dot{r}(t) - w|(\dot{r}(t) - w)$$

$$r(t, C) = \frac{1}{\frac{A}{m}C\rho\sigma}\log\left(1 + \frac{A}{m}C\rho\sigma(v_0 - w)t\right) + wt + r_0$$

physics-informed machine learning

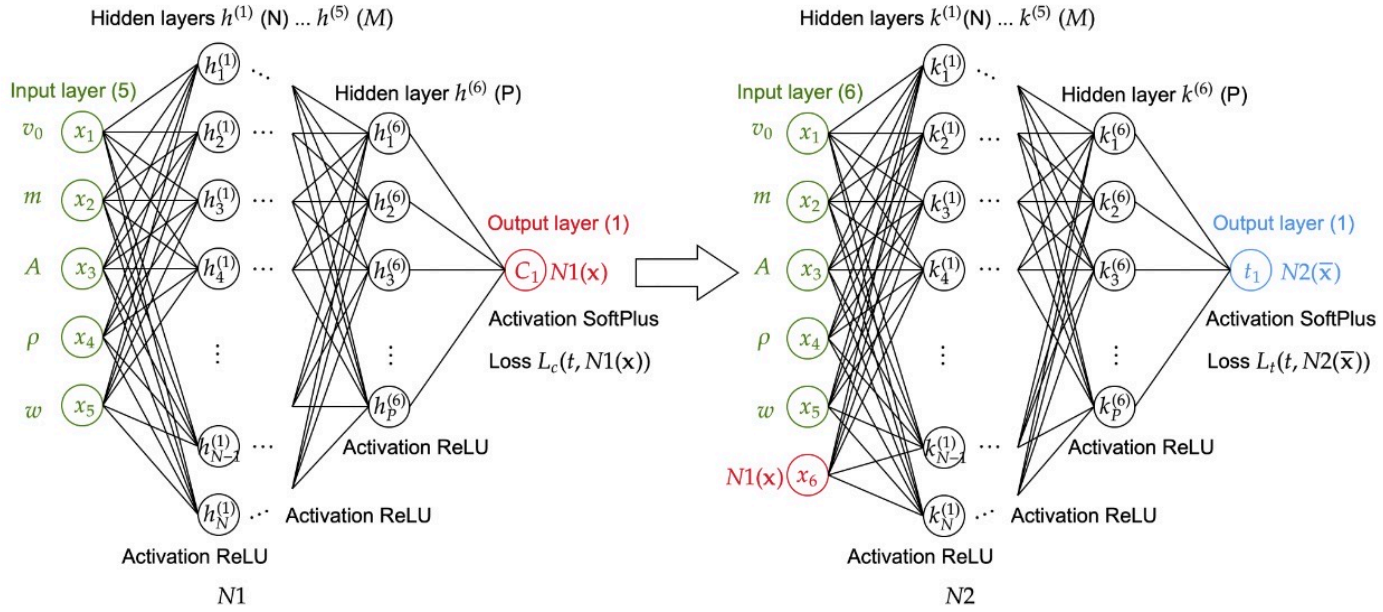

Configuration	Training phase			Testing phase
	$N1$	$N2$	λ	drag parameter as input of $N2$
C1	off	on	1	off
C2	on	on	0.5	off
C3	on	on	0	off
C4	on	on	1	on
C5	on	on	0.5	on
C6	on	on	0	on

$$L_c(t, N1(\mathbf{x})) = (r(t, N1(\mathbf{x})) - 1)^2 = \left(\frac{m\sigma}{A\rho N1(\mathbf{x})} \log\left(1 + \sigma \frac{A\rho N1(\mathbf{x})}{m}(v-w)t + wt\right) + r_0 - 1 \right)^2$$

$$L_t(t, N2(\bar{\mathbf{x}})) = \lambda(t - N2(\bar{\mathbf{x}}))^2 + (1-\lambda)(r(N1(\mathbf{x}), N2(\bar{\mathbf{x}})) - 1)^2$$

$$= \lambda(t - N2(\bar{\mathbf{x}}))^2 + (1-\lambda)\left(\frac{m\sigma}{A\rho N1(\mathbf{x})} \log\left(1 + \sigma \frac{A\rho N1(\mathbf{x})}{m}\right)(v-w)N2(\bar{\mathbf{x}})) + vN2(\bar{\mathbf{x}})) + r_0 - 1 \right)^2$$

prediction results

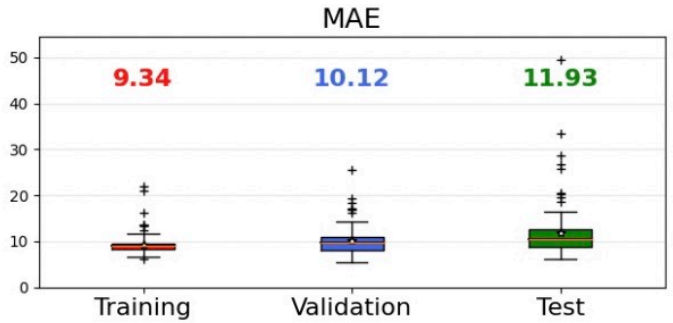

(a) C1

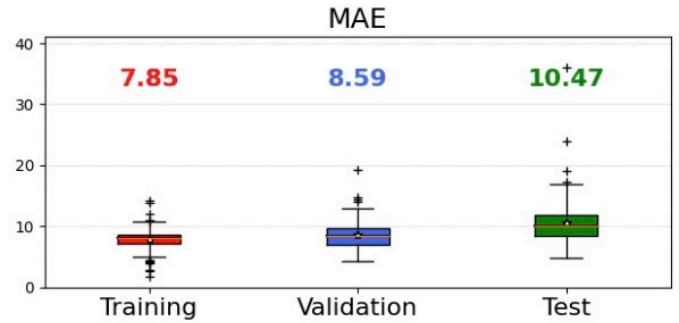

(b) C4

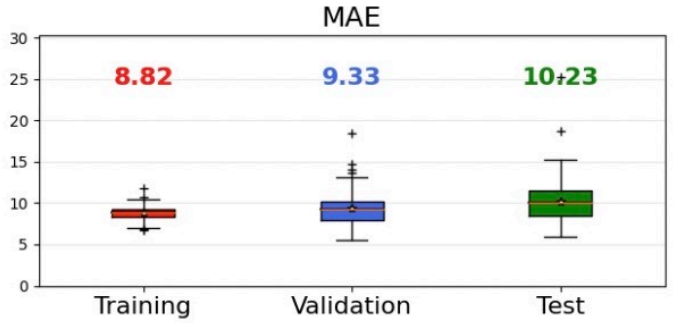

(c) C2

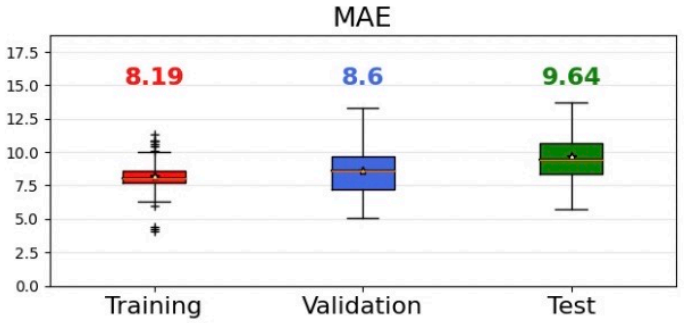

(d) C5

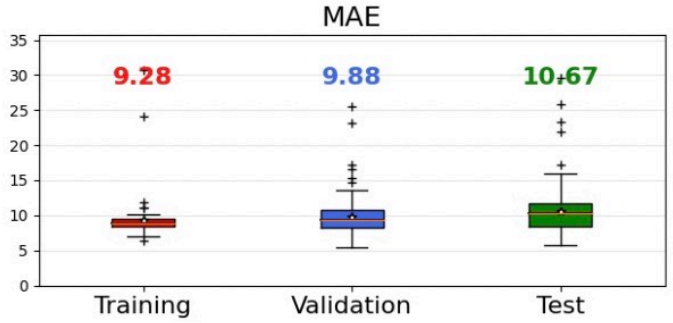

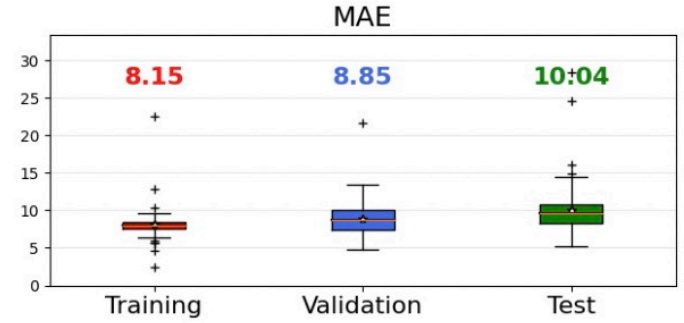

prediction results

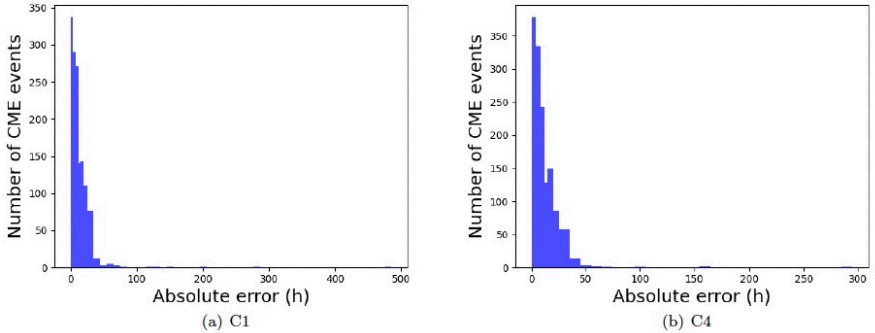

(a) C1

(b) C4

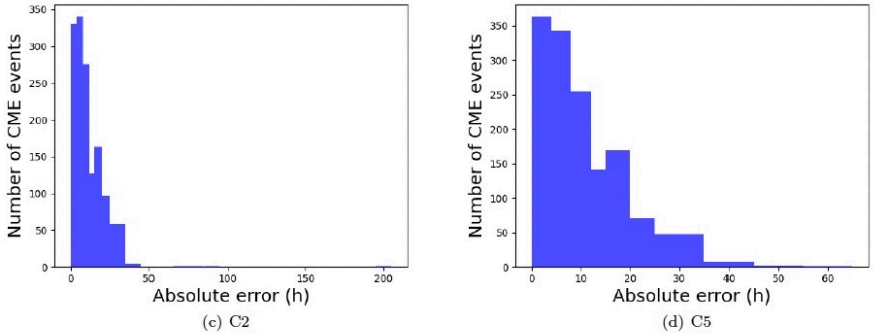

(c) C2

(d) C5

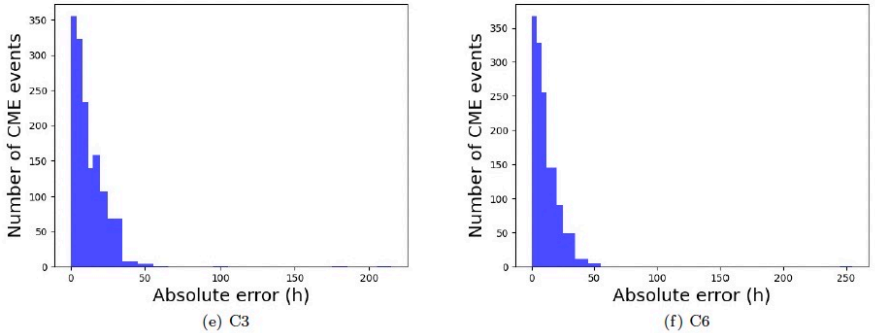

(e) C3

(f) C6

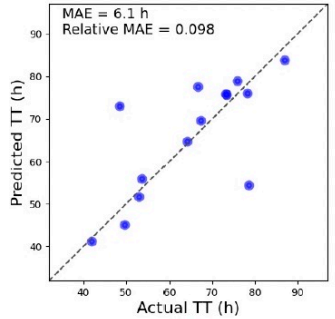

(a) C1

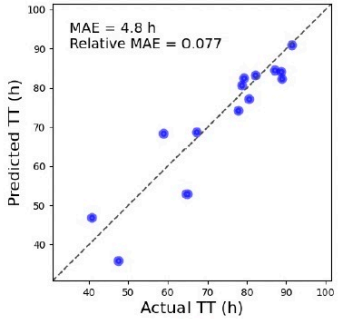

(b) C4

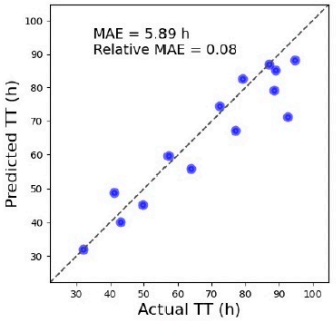

(c) C2

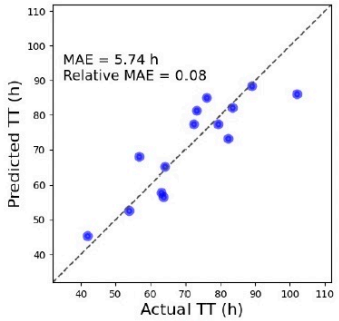

(d) C5

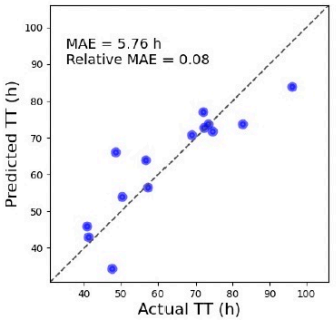

(e) C3

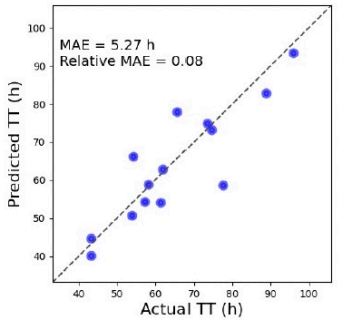

(f) C6

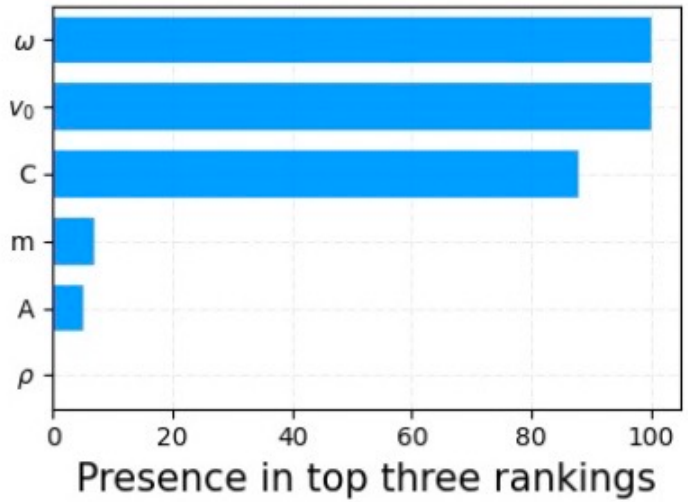

work in progress

- assessment of results by means of value-weighted skill scores
- value-weighted skill scores incorporated in score-oriented loss functions

- **marchetti f et al** 2022 score-oriented loss (sol) functions *pattern recognition* **132** 108913
- **guastavino s et al** 2022 bad and good errors: value-weighted skill scores in deep ensemble learning IEEE transactions on neural networks and learning systems

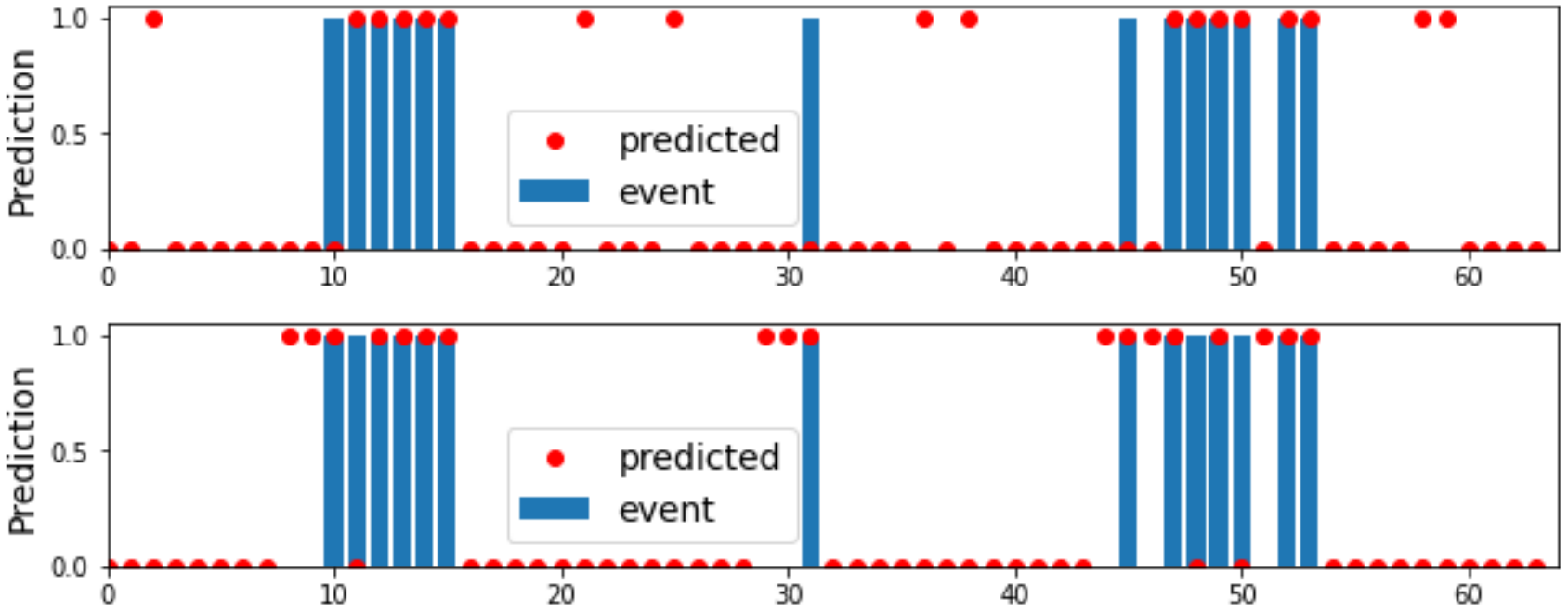

same TSS!
TSS=0.6457

references

- **guastavino s et al** 2022 operational solar flare forecasting via video-based deep learning *frontiers in astronomy* 9 2022
- **marchetti f et al** 2022 score-oriented loss (sol) functions *pattern recognition* **132** 108913
- **guastavino s et al** 2022 bad and good errors: value-weighted skill scores in deep ensemble learning IEEE transactions on neural networks and learning systems
- **campi c et al** 2019 feature ranking of active region source properties in solar flare forecasting and the uncompromised stochasticity of flare occurrence *astrophysical journal* **883** 150
- **guastavino s et al** 2022 implementation paradigm for supervised flare forecasting studies: A deep learning application with video data *astronomy and astrophysics* **662** A105
- **cicogna et al** 2021 flare forecasting algorithms based on high-gradient polarity inversion lines in active regions *astrophysical journal* **915** 38
- **the FLARECAST team** 2021 the flare likelihood and region eruption forecasting (FLARECAST) project: flare forecasting in the big data & machine learning era *journal of space weather and space climate* **11** 39
- **benvenuto f et al** 2018 a hybrid supervised/unsupervised machine learning approach to solar flare prediction *astrophysical journal* **853** 90
- **florios k et al** 2018 forecasting solar flares using magnetogram-based predictors and machine learning *solar physics* **293** 1

we are hiring people

please visit

https://mida.unige.it/form/open-positions

or write an email to

michele.piana@unige.it

Università di Genova

OSPEDALE POLICLINICO SAN MARTINO
Sistema Sanitario Regione Liguria

thank you!

e-mail: **piana@dima.unige.it**

MIDA Group | università di genova, Italy

More details available in: mida.unige.it

Università di Genova